



**HAL**  
open science

# A Generalised Approach to the Calibration of Orthotropic Materials for Thermoelastic Stress Analysis

T.R. Emery, J.M. Dulieu-Barton, J.S. Earl, P.R. Cunningham

► **To cite this version:**

T.R. Emery, J.M. Dulieu-Barton, J.S. Earl, P.R. Cunningham. A Generalised Approach to the Calibration of Orthotropic Materials for Thermoelastic Stress Analysis. *Composites Science and Technology*, 2009, 68 (3-4), pp.743. 10.1016/j.compscitech.2007.09.002 . hal-00550275

**HAL Id: hal-00550275**

**<https://hal.science/hal-00550275>**

Submitted on 26 Dec 2010

**HAL** is a multi-disciplinary open access archive for the deposit and dissemination of scientific research documents, whether they are published or not. The documents may come from teaching and research institutions in France or abroad, or from public or private research centers.

L'archive ouverte pluridisciplinaire **HAL**, est destinée au dépôt et à la diffusion de documents scientifiques de niveau recherche, publiés ou non, émanant des établissements d'enseignement et de recherche français ou étrangers, des laboratoires publics ou privés.

## Accepted Manuscript

A Generalised Approach to the Calibration of Orthotropic Materials for Thermoelastic Stress Analysis

T.R. Emery, J.M. Dulieu-Barton, J.S. Earl, P.R. Cunningham

PII: S0266-3538(07)00352-1  
DOI: [10.1016/j.compscitech.2007.09.002](https://doi.org/10.1016/j.compscitech.2007.09.002)  
Reference: CSTE 3823

To appear in: *Composites Science and Technology*

Received Date: 16 March 2007  
Revised Date: 31 August 2007  
Accepted Date: 6 September 2007

Please cite this article as: Emery, T.R., Dulieu-Barton, J.M., Earl, J.S., Cunningham, P.R., A Generalised Approach to the Calibration of Orthotropic Materials for Thermoelastic Stress Analysis, *Composites Science and Technology* (2007), doi: [10.1016/j.compscitech.2007.09.002](https://doi.org/10.1016/j.compscitech.2007.09.002)

This is a PDF file of an unedited manuscript that has been accepted for publication. As a service to our customers we are providing this early version of the manuscript. The manuscript will undergo copyediting, typesetting, and review of the resulting proof before it is published in its final form. Please note that during the production process errors may be discovered which could affect the content, and all legal disclaimers that apply to the journal pertain.



**A Generalised Approach to the Calibration of Orthotropic Materials for Thermoelastic Stress****Analysis****T R Emery<sup>a</sup>, J M Dulieu-Barton<sup>b\*</sup>, J S Earl<sup>c</sup> and P R Cunningham<sup>d</sup>**<sup>a</sup>trystan@soton.ac.uk, <sup>b</sup>janice@soton.ac.uk, <sup>c</sup>Jacqui.Earl@btinternet.com<sup>a, b, c</sup> School of Engineering Sciences, University of Southampton, SO17 1BJ, UK.<sup>d</sup>p.cunningham@lboro.ac.uk<sup>d</sup> Department of Aeronautical and Automotive Engineering, Loughborough University, Leicestershire, LE11 3TU, UK.**Abstract**

A review of thermoelastic theory associated with orthotropic solids is provided, the purpose of which is to develop a calibration procedure for thermoelastic stress analysis (TSA) that can be applied to laminated orthotropic composite materials. The procedure is based on the laminate strains rather than the surface ply stresses and enables a calibration approach that accounts simultaneously for the laminate mechanical response and the surface thermoelastic response. This calibration routine enables quantitative values of strain to be derived from thermoelastic data obtained from laminated composite structures. The calibration procedure is based on the use of simple tensile specimens. A variety of laminate stacking sequences are studied using E-glass epoxy pre-impregnated materials. Detailed material properties are obtained and the calibration procedure validated experimentally and theoretically.

**Keywords** Thermoelastic Stress Analysis; A. Polymer-matrix composites (PMCs); B. Thermomechanical properties; C. Laminate theory

**1. Introduction**

Thermoelastic Stress Analysis (TSA) is a well established technique for the evaluation of stresses in engineering components, e.g. [1-4]. To date most quantitative studies have concentrated on isotropic materials and the underlying theory has recently been summarised in a review [5]. Essentially an infra-red detector is used to measure the small temperature change associated with the thermoelastic effect [6] and is

related to the changes in the sum of the principal stresses on the surface of the material,  $\Delta(\sigma_x + \sigma_y)$ , [6] as follows:

$$\Delta T = -\frac{\alpha T_0}{\rho C_p} \Delta(\sigma_x + \sigma_y) \quad (1)$$

where  $\alpha$  is the coefficient of linear thermal expansion,  $T_0$  is the absolute temperature,  $\rho$  is the density,  $C_p$  is the specific heat at constant pressure and the subscripts  $x$  and  $y$  denote the directions of the principal stresses.

The output from the detector is termed the ‘thermoelastic signal’,  $S$ , and is related to the changes in the sum of the principal stresses on the surface of the material using the following expression:

$$\Delta(\sigma_x + \sigma_y) = AS \quad (2)$$

where  $A$  is a calibration constant.

Eq. (2) is valid for any linear elastic, isotropic, homogeneous material, assuming that the thermoelastic temperature change takes place under isentropic conditions. Techniques for obtaining the calibration constant for isotropic materials are well established; some common approaches have been described and assessed in Ref [7]. These involve either measuring the surface strains and relating them to the stresses or using a calibration test specimen with a known stress field. Techniques based on these calibration approaches are currently being developed into a standard for TSA measurements [8]. The simple thermoelastic theory devised for an isotropic body is not valid for orthotropic composite materials [9]. For orthotropic materials the following equation is used [9]:

$$(\alpha_1 \Delta \sigma_1 + \alpha_2 \Delta \sigma_2) = A^* S \quad (3)$$

where  $\alpha$  is the coefficient of linear thermal expansion and  $\Delta \sigma$  is the change in the direct surface stress,  $A^*$  is a further calibration constant and the subscripts 1 and 2 denote the principal material directions of the surface lamina.

Stanley and Chan [9] validated Eq. (3) using two types of composite component. Potter [10] proposed a thermoelastic theory relating the thermoelastic output to that of the surface strains and demonstrated its validity on a carbon fibre / epoxy resin laminate. Bakis and Reifsnider [11] investigated

the influence of material inhomogeneity and anisotropy using carbon fibre reinforced plastics. They also investigated the limitations of Eq. (3) in terms of adiabatic thermoelastic assumption made in its development. It was found that the thermoelastic response was affected by a number of factors, which included the volume fraction, the thermoelastic properties of the micro-constituent materials, the orientations of the laminae within the laminate, and the orientation of the lamina on the surface. For composite materials it was suggested that the non-adiabatic behaviour in CFRP laminates could be due to heat transfer between the fibre and matrix or caused by viscoelastic effects. The former was discounted [12] for fibres of diameter  $\approx 7 \mu\text{m}$  which is typical for carbon fibres. Wong [12] discussed the effects of non-adiabatic conditions on the thermoelastic signal recorded from the specimen surface due to heat transfer characteristics at large stress gradients, such as those experienced between plies orientated at different angles in a laminate. Cunningham et al [13] have shown that in glass reinforced epoxy composites the adiabatic assumption is valid. This was also confirmed in a study on pultruded composite materials [14]. Pitarresi et al [15] studied woven composite material and concluded that the thermoelastic response was generated by strain transfer into the resin-rich surface layer. A number of quantitative studies have been carried out on composite structures [16-18] by deriving a calibration constant; however a generalised calibration routine has not been developed. Therefore it is not possible at present to apply TSA in a straightforward manner to a general composite structure and obtain quantitative stress or strain values. As the TSA technique can collect data from the actual structure under fatigue type loading a clear benefit of a calibration strategy would be to link the thermoelastic response with failure. This would provide a route for comparison with existing failure theories such as those described by Daniel [19] and the potential to develop a new damage assessment procedure based on the thermoelastic response.

Eq. (3) states that the thermoelastic response from a laminated composite is dependent on the stress in the surface lamina and neglects the resin-rich layer. The stress in the surface ply and the resin-rich layer is dependent on the architecture of the composite construction, i.e. the stacking sequence of the laminae that form the laminate. If the elastic properties of the lamina, the thickness of the manufactured ply and the load are known it is possible to calculate the stress in the surface lamina or the resin-rich layer. This would provide a route to calibration but is laden with possible sources of error due to estimates of material properties etc. A better approach is to formulate Eq. (3) in terms of strain and use this as a basis for

calibration, as under in-plane loading the strain is constant through the thickness of a multidirectional laminate and can be measured using extensometers or strain gauges. In [10, 13, 14, 15] strain formulations are used to assess the thermoelastic response for specific materials, but the issue of calibration is not addressed. The objective of the present work is to devise a general calibration routine for orthotropic composite laminates based upon laminate strains rather than the surface lamina stresses. In doing this it is possible to include the resin-rich surface layer in the analysis and establish if the response is from the orthotropic surface ply or the isotropic resin-rich layer as suggested in [13 - 15].

The calibration routine is validated using a variety of multidirectional laminates constructed from layers of UD pre-impregnated glass fibre reinforced epoxy. These are made into a series of standard tensile specimens with similar surface ply properties but with different global stiffness and Poisson's ratio values. The tensile specimen was chosen as it provides a simple in-plane loading where the stress in each ply can be calculated. It is important to note that only symmetrical lay-ups were used, as this avoids any out-of-plane deformation and further simplifies the calibration procedure. However, it should be stressed that the derived calibration constant can be applied to components that are experiencing out-of-plane deformation. In the present work  $A^*$  is obtained for the material using three approaches: (i) using Eq. (3) and *calculating* the surface ply or resin-rich layer *stresses* using Classical Laminate Theory (CLT) [20], (ii) *calculating* the laminate *strains* using CLT [20], and (iii) *measuring* the laminate *strains*.

In each case the measured thermoelastic signal is combined with the stresses/strain to give  $A^*$ . For (ii) and (iii) it was necessary to develop new formulations, which are provided in the paper. To generate these formulations it was necessary to revisit the thermoelastic theory for orthotropic materials. Therefore a background to the development of Eq. (3) is provided in the theory section of the paper along with a representation of Potter's original formulation [10] in terms of the thermoelastic signal,  $S$ , and the development of the theory for the calibration procedure. The test specimens were loaded with constant stress and constant displacement. The thermoelastic data from each specimen under each loading condition are used to obtain  $A^*$  using each of the three calibration approaches. In validating the values of  $A^*$  it is demonstrated that the response from the test specimens is not from the orthotropic surface ply but from the thin (~25  $\mu\text{m}$ ) surface resin layer. Experimental evidence is provided in the paper that confirms the findings of earlier work [13-15] in a quantitative manner.

## 2. Theory

Over the past two decades many researchers have generated theory to relate the thermoelastic signal to that of the stress state in a loaded orthotropic material, e.g. [9]. In this paper the theory is developed in terms of strain instead of stress. The first step in this approach is to recognise that in thermoelastic analyses of laminated composites there are three stress/strain systems that must be considered as follows:

- (a) in the individual plies, relative to the lamina principal directions, denoted by the subscripts 1 and 2 (for TSA the surface lamina is most important)
- (b) in the individual plies, relative to the direction of the principal stress, denoted by the subscripts  $x$  and  $y$  (again, for TSA the surface lamina is most important)
- (c) in the laminate, relative to the laminate principal material directions, denoted L and T (this allows the global mechanical response of the material to be included in the assessment of the thermoelastic response).

The starting point for the theory is the standard stress and strain relationship for an orthotropic lamina [20] that includes the thermal expansion terms. In orthotropic materials there is no interaction between normal stresses  $\sigma_1, \sigma_2, \sigma_3$ , and shear strains  $\gamma_4, \gamma_5, \gamma_6$ , no interaction between shear stresses  $\tau_4, \tau_5, \tau_6$ , and normal strains  $\varepsilon_1, \varepsilon_2, \varepsilon_3$  and no interaction between shear stresses and shear strains in different lamina. Furthermore a single ply of composite material, i.e. a lamina, and can be considered as in a plane stress condition, so that  $\sigma_3 = \tau_4 = \tau_5 = 0$ . Also in the principal material directions a thermal expansion does not produce a shear deformation. Therefore the stresses in the lamina are related to the strains as follows:

$$\begin{bmatrix} \sigma_1 \\ \sigma_2 \\ \tau_6 \end{bmatrix} = \begin{bmatrix} Q_{11} & Q_{12} & 0 \\ Q_{12} & Q_{22} & 0 \\ 0 & 0 & Q_{66} \end{bmatrix} \begin{bmatrix} \varepsilon_1 - \alpha_1 \Delta T \\ \varepsilon_2 - \alpha_2 \Delta T \\ \gamma_6 \end{bmatrix} \quad (4)$$

where  $\varepsilon_1, \varepsilon_2$  and  $\gamma_6$  are the strains in the material fibre direction and the reduced stiffness values are as

follows:  $Q_{11} = E_1 / (1 - \nu_{12}\nu_{21})$ ,  $Q_{22} = E_2 / (1 - \nu_{12}\nu_{21})$ ,  $Q_{12} = \nu_{21}E_1 / (1 - \nu_{12}\nu_{21}) = \nu_{12}E_2 / (1 - \nu_{12}\nu_{21})$  and  $Q_{66} = G_{12}$ .

Likewise the strains can be formulated in terms of the stresses as follows:

$$\begin{bmatrix} \varepsilon_1 \\ \varepsilon_2 \\ \gamma_6 \end{bmatrix} = \begin{bmatrix} S_{11} & S_{12} & 0 \\ S_{21} & S_{22} & 0 \\ 0 & 0 & S_{66} \end{bmatrix} \begin{bmatrix} \sigma_1 \\ \sigma_2 \\ \tau_6 \end{bmatrix} + \begin{bmatrix} \alpha_1 \\ \alpha_2 \\ 0 \end{bmatrix} [\Delta T] \quad (5)$$

where the compliance terms are defined as;  $S_{11} = \frac{1}{E_1}$ ,  $S_{22} = \frac{1}{E_2}$ ,  $S_{12} = \frac{-\nu_{12}}{E_1} = \frac{-\nu_{21}}{E_2}$  and  $S_{66} = \frac{1}{G_{12}}$ .

The thermoelastic relationship for the temperature change,  $\Delta T$ , caused by a change in the stress state in a linear elastic, homogeneous solid is derived from the laws of thermodynamics in the form [6]

$$\Delta T = -\frac{T}{\rho C_\varepsilon} \sum_i \frac{\partial \sigma_i}{\partial T} \varepsilon_i + \frac{q}{\rho C_\varepsilon}, \text{ with } i = 1, \dots, 6 \quad (6)$$

where  $T$  is the absolute temperature,  $C_\varepsilon$  is the specific heat at constant strain,  $q$  is the heat input,  $\rho$  is the mass density,  $\sigma_i$  is the stress change tensor and  $\varepsilon_i$  is the strain change tensor referred to a system of Cartesian coordinate axes.

The thermal conductivity of polymers such as those used in composite laminate is practically zero. It has also been shown experimentally that for GRP materials adiabatic behaviour prevails [13-14]. Therefore to simplify matters the heat input term in Eq. (6) is neglected, so adiabatic conditions can be assumed.

Therefore for an orthotropic in-plane lamina the basic thermoelastic relationship (Eq. (6)) can be rewritten in terms of the lamina compliance terms. This is achieved by differentiating Eq. (4) (assuming that the elastic constants are independent of temperature) and substituting in to Eq. (6) and by substituting the strain terms from Eq. (5) into Eq. (6) as follows

$$\begin{aligned} \Delta T = -\frac{T}{\rho C_\varepsilon} \{ & (Q_{11}\alpha_1 + Q_{12}\alpha_2)(S_{11}\sigma_1 + S_{12}\sigma_2 + \alpha_1\Delta T) \\ & + (Q_{12}\alpha_1 + Q_{22}\alpha_2)(S_{21}\sigma_1 + S_{22}\sigma_2 + \alpha_2\Delta T) \} \end{aligned} \quad (7)$$

To further simplify, the next step is to derive a relationship between  $C_\varepsilon$  and  $C_p$  (the specific heat at constant pressure). This relationship between  $C_p$  and the specific heat at constant volume is [21]:

$$C_p - C_v = T \left( \frac{\partial P}{\partial T} \right)_v \left( \frac{\partial V}{\partial T} \right)_p \quad (8)$$

and introducing  $C_\varepsilon$  requires that the density be included as follows:

$$C_p - C_\varepsilon = -\frac{T}{\rho} \left( \frac{\partial \sigma_i}{\partial T} \right) \left( \frac{\partial \varepsilon_i}{\partial T} \right) \quad (9)$$

Assuming the elastic constants are temperature independent over the temperature range of interest, the specific heat at constant strain,  $C_\varepsilon$ , can be rewritten in terms of the specific heat at constant pressure,  $C_p$ , by

making the substitution  $C_\varepsilon = \frac{T}{\rho} \{ Q_{11}\alpha_1^2 + 2Q_{12}\alpha_1\alpha_2 + Q_{22}\alpha_2^2 \} + C_p$  into Eq. (7) so that the following

familiar expression is obtained:

$$\Delta T = -\frac{T}{\rho C_p} (\alpha_1 \Delta \sigma_1 + \alpha_2 \Delta \sigma_2) \quad (10)$$

In TSA  $\Delta T$  is measured using a highly sensitive infra-red detector.  $\Delta T$  produces a voltage output from the detector which is processed to produce a digital signal, i.e. the thermoelastic signal,  $S$  (see Eq. (3)). Combining the detector properties, the surface properties and the processing parameters from the analogue to digital converter with quantities outside the brackets on the right hand side of Eq. (10) provides the calibration constant,  $A^*$ . This procedure results in the equation given by Eq. (3). In developing the procedure it is assumed that the surface temperature remains constant throughout the calibration test; this is valid as the data collection time is of the order of a few seconds. However, it is essential that the temperature at which the calibration was performed is recorded, as this will most likely be different to that during TSA measurement of the component. It is necessary to temperature correct the data from the test so that it is compatible with the temperature during the calibration. To do this a temperature correction procedure has been developed by the authors [22] that can be incorporated into the calibration analysis routine. From Eq. (7) a thermoelastic equation is derived in terms of the lamina strains as follows:

$$\Delta T = -\frac{T}{\rho C_\varepsilon} \{ (Q_{11}\alpha_1 + Q_{12}\alpha_2) \Delta \varepsilon_1 + (Q_{12}\alpha_1 + Q_{22}\alpha_2) \Delta \varepsilon_2 \} \quad (11)$$

It is now possible to develop a thermoelastic equation similar to that given by Eq. (3) in terms of the lamina strains. For convenience it is assumed that for a solid material  $C_p$  and  $C_\varepsilon$  are equal so that the constant  $A^*$  can be included as follows:

$$A^* S = (\alpha_1 Q_{11} + \alpha_2 Q_{12}) \Delta \varepsilon_1 + (\alpha_1 Q_{12} + \alpha_2 Q_{22}) \Delta \varepsilon_2 \quad (12)$$

The strain in the surface ply fibre direction can be related to the strain in the laminate principal material directions (i.e.  $L$  and  $T$  directions) with the expression:

$$[\varepsilon]_{1,2} = [T][\varepsilon]_{L,T} \quad (13)$$

where  $[T]$  is the standard transformation matrix [20].

By substituting Eq. (13) into Eq. (12) a thermoelastic equation is obtained in terms of the laminate longitudinal,  $L$ , and transverse,  $T$ , strains, i.e.:

$$\begin{aligned} A^* S = & \left\{ [(\alpha_1 Q_{11} + \alpha_2 Q_{12})m^2 + (\alpha_1 Q_{12} + \alpha_2 Q_{22})n^2] \Delta \varepsilon_L \right. \\ & + [(\alpha_1 Q_{11} + \alpha_2 Q_{12})n^2 + (\alpha_1 Q_{12} + \alpha_2 Q_{22})m^2] \Delta \varepsilon_T \\ & \left. + [(\alpha_1 Q_{11} + \alpha_2 Q_{12})mn - (\alpha_1 Q_{12} + \alpha_2 Q_{22})mn] \Delta \gamma_{LT} \right\} \end{aligned} \quad (14)$$

where  $m = \cos \theta$  and  $n = \sin \theta$  ( $\theta$  is the angle between the axes of the surface ply (1, 2) and those of the laminate ( $L$ ,  $T$ )). The expression given by Eq. (14) is the basis for the calibration procedure. The equation can be simplified by judicious choice of stacking sequence, specimen geometry and loading configuration as shown in the next section of the paper.

### 3. Calibration Test Specimens

The composite material used for the test specimens was 13 layers of a unidirectional E-glass epoxy (SE84) pre-impregnated material. The panels were consolidated under vacuum pressure for one hour and then cured for four hours at a temperature of 80 °C. After curing, end tabs strips were bonded to both sides of the panel using an adhesive film. Five panels were made with different stacking sequences, as detailed in Table 1. The tabs were manufactured of the same material with 17 layers and a  $[0]_{17}$  lay-up. The tabs were tapered at an angle of 15°, which provided a 15mm scarf. The end tabbed panels were then cut into tensile type test specimens of the configuration shown in Fig. 1, as recommended by the ASTM standard Ref. [23]. The specimens were 40 mm wide with an approximate length between the flat faces of the end tabs of 180 mm and thickness 3.5 mm respectively. The laminate plates, from which the specimens were cut, were manufactured individually and the slight variations in the finished geometry of the specimens

were measured. The thickness and length between the end tabs of the specimens, which are important metrics in the subsequent analysis of the laminates, are given in Table 1. Fig. 2 shows a micrograph of a section of the specimen close to the surface. The surface resin-rich layer is indicated in Fig. 2 and is approximately 25  $\mu\text{m}$  thick (approximately the size of a fibre diameter).

In Fig. 1 a 45° surface ply is shown. The surface ply axes (1, 2), laminate axes (L, T) and principal stress axes (x, y) are also shown in Fig. 1. The specimen loading is also provided in Fig. 1. The five laminate configurations given in Table 1 are denoted as follows: ‘UD’ for a *unidirectional laminate* i.e. all plies in the longitudinal direction, ‘Mixed’ for a laminate with only two transverse plies and a longitudinal surface ply, ‘0/90’ for a *cross-ply laminate* with a longitudinal surface ply, ‘90/0’ for a *cross-ply laminate* with a transverse surface ply and ‘ $\pm 45$ ’ for an *angle-ply laminate* with a surface ply at 45° to the longitudinal direction. The UD, Mixed and 0/90 specimens were manufactured to allow thermoelastic analysis of specimens that have the same surface properties and different mechanical properties. The 0/90 and 90/0 specimens allowed evaluation of materials that have different surface properties but similar mechanical properties. The angle-ply laminate, i.e.  $\pm 45$ , was included as it has a finite laminate shear strain. In all cases the principal stress axes (x, y) are coincident with the laminate axes (L, T), i.e. the first principal stress direction is always the laminate longitudinal direction. The specimens used here complement the carbon fibre epoxy specimens used by Potter [10] and also add the feature of varying the surface ply orientation.

To obtain the calibration constant,  $A^*$ , from the test specimens described above using Eq. (14), it is necessary to derive equations for each specimen that are functions of the laminate principal strains. In a tensile test specimen the transverse strain in the laminate is related to the longitudinal strain by  $\epsilon_T = -\nu_{LT}\epsilon_L$ , where  $\nu_{LT}$  is the laminate major Poisson’s ratio. Therefore it is possible to eliminate  $\epsilon_T$  from Eq. (14) for a tensile specimen (with the exception of the  $\pm 45$  specimen) and express  $A^*$  as a function of the longitudinal strain alone. The orientation of the surface ply fibre direction is relative to the longitudinal laminate axes, and denoted as  $\theta$ , see Fig. 1. The UD, Mixed and 0/90 laminates have a surface fibre direction coincident with the laminate axes and as such  $\theta$  is equal to zero. Therefore the calibration equation for these three laminates is identical and involves only the  $n^2$  term given in Eq. (14). The 90/0 has

a surface fibre direction orientated at  $90^\circ$  to the laminate longitudinal axes and as such the calibration equation is a function of only the  $m^2$  terms in Eq. (14). For angle ply laminates such as the  $\pm 45$ , where the direction of the surface fibre orientation is somewhere between  $0^\circ$  and  $90^\circ$ , the calibration equation is a product of both the  $m^2$ ,  $n^2$  and  $mn$  terms, meaning that the shear term  $\gamma_{LT}$  is retained. It is important to note that the strain terms,  $\varepsilon_L$ ,  $\varepsilon_T$  and  $\gamma_{LT}$ , in the equations given in Table 1 are, by strain compatibility, constant through the thickness of the laminate. In Table 1 the expressions are provided for  $A^*$  for each of the specimens. The last row in Table 1 gives the calibration constant based on the response from the resin-rich layer for each of the specimens and varies only with  $\nu_{LT}$ .

To calculate the calibration constant,  $A^*$ , from each specimen type given in Table 1 a test programme was devised to gather the required data in the two manners described in the introduction; experimentally using measured values and numerically using calculated values.  $A^*$  was also calculated for each laminate using the traditional stress formulation as given by Eq. (3). For all cases the thermoelastic signal,  $S$ , was recorded from each laminate. Once the full compliment of terms on the right-hand side of the equations have been determined the calibration constant,  $A^*$ , can be evaluated. By inspection of Eq. (3) and Eq. (10) it can be seen that  $A^*$  is a function of the density and the specific heat only. If the same detector is used, the same surface preparation is carried out and the temperature remains constant then  $A^*$  is independent of the surface ply orientation. Therefore each of the equations given in Table 1 should yield the same value of  $A^*$ . Likewise,  $A^*$  obtained from the stress formulation should be identical to that obtained from the strain formulations provided in Table 1.

#### 4. Derivation of the parameters for calibration

##### 4.1 Loading regimes

The test specimens were gripped along the entire tab length (see Fig. 1) and cyclically loaded in an Instron 8802 test machine. The loading frequency was 10 Hz, which has been shown [13] to be sufficient to generate adiabatic conditions in the test specimens. Two data sets were generated: one where the load range was constant at 8 kN and one where the displacement range was constant at 0.44 mm for each of the five test specimens. The variation in strain for the specimens loaded with a constant load would be expected to vary significantly because of the variation in laminate stiffness, whereas the specimens loaded

with a constant displacement might be expected to provide constant strain values. However, this was not the case and the limitations of displacement control are discussed in Section 4.4. The displacement resulting from the constant applied load of 8 kN and the load resulting from the constant applied displacement of 0.44 mm were also recorded at the time of the test and are provided in Table 2.

#### 4.2 Material Properties

In order to evaluate  $A^*$  from the equations in Table 1 it is necessary to establish the properties for the laminate constituent material and the resin-rich layer. The laminate constituent material properties can be divided in two categories; *i*) those relating to the surface lamina, i.e.  $\alpha_1$ ,  $\alpha_2$ ,  $Q_{11}$ ,  $Q_{22}$ , and  $Q_{12}$ , are surface ply properties in the principal material directions and *ii*) those relating to the global behaviour of the laminate, in this case,  $\nu_{LT}$ .

The mechanical properties required for the calculation of the reduced stiffness terms, (namely  $E_1$ ,  $E_2$ ,  $G_{12}$ ,  $\nu_{12}$  and  $\nu_{21}$ ) and the major Poisson's ratio value,  $\nu_{LT}$ , were obtained from experimental studies of unidirectional test specimens. To determine these values orthogonal strains were obtained from two UD laminates loaded in tension. The first laminate had its fibres orientated longitudinally, i.e. at  $0^\circ$  and the second with the fibres orientated transversely, i.e. at  $90^\circ$ . Two extensometers were used of gauge length 50mm in the longitudinal direction and 40mm in the transverse direction to obtain strain values from the mid section of the specimens. The material properties for the laminate are given in Table 3. The values calculated from these UD laminates can be expected from a single UD lamina and form the basis of the calculation of  $Q_{11}$ ,  $Q_{22}$ , and  $Q_{12}$ . The shear modulus and the coefficients of thermal expansion are detailed in Table 3 and were taken from values presented in literature [24, 25]. Material properties for the epoxy layer obtained from the manufacturers/literature [26, 27, 28] for similar materials used in composite manufacture are given in Table 4.

The major Poisson's ratio,  $\nu_{LT}$ , for each of the test specimens is required for the strain calibration equations, in Table 1. The major Poisson's ratio,  $\nu_{LT}$ , can be calculated for each of the test specimens using CLT with the geometry, stacking sequence, ply orientation and ply material properties. The calculation of Poisson's ratio also enables the Young's moduli values for each of the test specimens to be evaluated. Whilst these values are not explicitly required for the thermoelastic calibrations given in Table 1 they have

been calculated so that the CLT results can be compared against experimentally determined values, and thus provide a confirmation of the CLT values (see Table 5). The experimental results, for the laminate elastic properties, were obtained in an identical manner to those described to obtain the material characteristics of a UD lamina (see above). The results for the  $\nu_{LT}$  and  $E_L$  values for the test specimens are given in Table 5. (The first two rows of data repeat the results obtained previously for the two UD laminates tested.) There is good agreement between these sets of data, giving confidence in the CLT methodology and the stress and strains derived from this (see below), as well as validating the calculated elastic properties for each laminate.

#### 4.3 Calculation of strains and stresses

The remaining unknown terms are the laminate strains, surface ply stresses and thermoelastic signal. The stresses,  $\Delta\sigma_1$  and  $\Delta\sigma_2$ , are calculated using CLT [20] whilst the strains,  $\Delta\epsilon_L$ ,  $\Delta\epsilon_T$  and  $\Delta\gamma_{LT}$  are also calculated using CLT and obtained experimentally. The CLT calculations required for each of the test specimens are repetitive in nature, so a computational procedure was developed to calculate the behaviour, as detailed by Daniel and Ishai [20]. The material properties and geometries required for these calculations follow those previously obtained and are provided in Tables 1-4. The strains were derived using CLT in the  $L$  and  $T$  directions to input into the calibration equations in Table 1; these are provided in Table 6 and Table 7 for the load and displacement control tests respectively. These laminate strain values were then transformed so that they were expressed relative to the principal surface ply fibre directions, so that the stresses in the surface ply could be obtained. The stresses in the surface ply in the direction of the principal material axes are provided in Tables 6 and 7 for load and displacement control respectively.

#### 4.4 Measurement of laminate strain

During testing the displacement applied to the test specimens was accurately recorded during both the displacement and load control tests. Therefore using the gauge length of the specimen it is possible to estimate the strain in the specimens. However, this proved inaccurate due to the scarf of the end tab protruding beyond the gripped tab area, as shown in Fig. 1. As all the tabs were of a UD configuration and therefore the stiffness did not match the specimens (apart from the UD), so the strain in the specimens cannot be accurately determined from the applied displacement. Therefore the laminate applied strain

ranges ( $\Delta\epsilon_L$  and  $\Delta\epsilon_T$ ) were measured using a dynamic extensometer. The measured laminate applied strain is recorded in Tables 6 and 7 for load and displacement control respectively and it can be seen that these values correlate well with those calculated using CLT.

The stiffening effect of the scarf is demonstrated in Table 7 where it can be seen that the  $\Delta\epsilon_L$  values are not constant for the same applied displacement. Clearly taking the 0.44 mm displacement value and dividing by the gauge length would produce larger values of  $\Delta\epsilon_L$  than reported in Tables 6 and 7. From the stress data shown in Tables 6 and 7 it is evident that in the mixed, 0/90 and 90/0 there is a finite transverse stress in the specimens. This occurs as a consequence of the traction imposed by the mismatch in the Poisson's ratio ply by ply. The finite transverse stress value is significant as it is multiplied by  $\alpha_2$  in Eq. (3), and  $\alpha_2$  for a glass epoxy laminate is in the order of six times greater than  $\alpha_1$  (see Table 3).

#### 4.5 Thermoelastic signal

The last variable required to determine  $A^*$  is the thermoelastic signal,  $S$ . To record the thermoelastic signal from each of the test specimens each specimen was loaded as described in Table 2 at a frequency of 10 Hz. A Stress Photonics Deltatherm TSA system [29] was used to collect the thermoelastic data. A 25 mm infrared lens was used which determined the detector was positioned at a stand-off distance of 500 mm from the specimen surface to achieve a full-field of view of the test specimen. The specimen surface, from which the thermoelastic signal was recorded, was left in the manufactured state and unpainted as the epoxy surface provides a sufficiently high emissivity for thermoelastic studies. Inspection of the thermal data recorded simultaneously with the thermoelastic data showed no thermal variations between the test specimens during the tests so it was not necessary to correct the thermoelastic signal for temperature variations [22]. The thermoelastic signal recorded from both test regimes are detailed in uncalibrated A/D units in Tables 8 for the load and displacement control tests. The data had coefficients of variation in the range 4.5 % to 7.9 %. It can be seen from these tables that neither a constant applied load nor a constant applied displacement result in a constant thermoelastic signal. In general the thermoelastic signal magnitudes follow the order of the laminate longitudinal stiffness given in Table 5, with the exception of the  $\pm 45$ ; this is discussed in detail in the next section.

## 5. Validation of Calibration Routine

Using either the calculated or measured data it is now possible to obtain  $A^*$  from the three approaches described; *i*) using the calculated surface ply *stresses* given in Tables 6 and 7 and applying Eq. (3), *ii*) using the calculated laminate *strains* given in Tables 6 and 7 and applying Eq. (14) and *iii*) using the measured laminate *strains* and applying Eq. (14). The values for  $A^*$  are listed in Table 9 for the constant load tests and Table 10 for the constant displacement tests. In Tables 9 and 10 values of  $\nu_{LT}$  calculated from CLT were used in rows *i* and *ii* and measured values of  $\nu_{LT}$  were used in row *iii*. The value of  $A^*$  obtained using the orthotropic surface ply properties has an average value of  $0.589 \text{ MPa}^\circ\text{C} \pm 4.3 \%$  and  $0.578 \text{ MPa}^\circ\text{C} \pm 3.6 \%$  for the constant load and constant displacement tests respectively. Values of  $A^*$  are given in Tables 11 and 12, assuming that the resin-rich layer is the source of the thermoelastic signal. In this case  $A^*$  has an average value of  $0.801 \text{ MPa}^\circ\text{C} \pm 5.72 \%$  and  $0.772 \text{ MPa}^\circ\text{C} \pm 2.52 \%$  for the constant load and constant displacement tests respectively. (It should be noted that the values of  $A^*$  presented in Tables 9 - 12 are not absolute and are specific to the Deltatherm system, the system settings and the surface temperature and emissivity of the specimen.)

$A^*$  is a function only of the specific heat and density of the material and not dependent on the orthotropic properties of the laminate. Therefore the fact that the  $A^*$  values are in close agreement does not completely validate the theory presented here and does not identify if the signal response is from the resin-rich surface layer or the orthotropic surface ply. A further important feature is the difference between the values of  $(\alpha_1 Q_{11} + \alpha_2 Q_{12})$  and  $(\alpha_1 Q_{12} + \alpha_2 Q_{22})$  that appear in Eq. (14). For this material  $(\alpha_1 Q_{11} + \alpha_2 Q_{12})$  equals  $0.298 \text{ MPa}^\circ\text{C}$  and  $(\alpha_1 Q_{12} + \alpha_2 Q_{22})$  equals  $0.311 \text{ MPa}^\circ\text{C}$ . Clearly the difference between the response of the 0/90 and 90/0 specimen will be very small as indicated in Table 8. The values of  $(\alpha_1 Q_{11} + \alpha_2 Q_{12})$  and  $(\alpha_1 Q_{12} + \alpha_2 Q_{22})$  for the isotropic resin material are equal at  $0.4031 \text{ MPa}^\circ\text{C}$ . The difference between this value and that obtained for the orthotropic material of approximately  $0.30 \text{ MPa}^\circ\text{C}$  accounts for the factor of 25% difference between the two sets of  $A^*$  values.

To identify the source of the thermoelastic signal with certainty it was necessary to derive a value of  $\Delta T$  to ascertain if it is the orthotropic surface ply or the resin-rich layer that provides the response. The Deltatherm system is not radiometrically calibrated, therefore it is impossible to determine an absolute value of the thermoelastic temperature change as given by Eqs. (1) and (10). It was necessary to use an IR

system that is radiometrically calibrated and as such capable of resolving the temperature change associated with the thermoelastic response. Here a Cedip Silver IR system, with a temperature resolution of 17 mK was used to obtain  $\Delta T$ . The data required to evaluate  $\Delta T$  directly is given in Tables 3 and 4 for the orthotropic surface ply and resin-rich layer respectively. For the orthotropic material; the specific heat,  $C_p$ , value was obtained from [30] and the density measured [13]. The equivalent data for the epoxy material was obtained from literature [27, 30, 31]. Tables 14 and 15 provide calculated and measured  $\Delta T$  values using both the isotropic resin-rich layer and the orthotropic surface ply. The temperature of specimen surface remained constant through the testing and at a value of 291 K.

It is evident from Table 13 and Table 14 that the measured thermoelastic response is that of the resin-rich layer and not that from the orthotropic surface ply, as the measured  $\Delta T$  values are in close agreement with those calculated using material properties. This indicates that any composite material with a resin-rich layer of 25  $\mu\text{m}$  or greater can be treated as ‘thermoelastically isotropic’. However the material construction, i.e. the stacking sequence must be considered in any analysis and must be considered as ‘mechanically orthotropic’. Therefore a calibration routine must be devised that accounts for the mechanical orthotropy of the material, without the need to know the material properties laboriously derived in Section 4.2. Moreover this routine must be based on a strain measurement, rather than calculating the stress in the resin-rich layer. Such a calibration constant using a simple tensile specimen would be as follows:

$$\frac{\Delta \epsilon_L (1 - \nu_{LT})}{S} = \frac{A^* (1 - \nu_R)}{\alpha E_R} = B^* \quad (15)$$

Table 15 gives the  $B^*$  values for each test specimen and it can be seen the value is constant for the UD, Mixed, 0/90 and 90/0 the value is  $0.191 \pm 0.47\%$ . It can be seen that the  $\pm 45$  is about 20% greater than the other values. The explanation for this may result from discrepancies in the properties used for the  $\pm 45$ ; from Table 5 it can be seen that there is a difference between the calculated and measured values and also the shear modulus was obtained from literature sources.

Having derived  $B^*$  it is now possible to relate the sum of the principal strains to the thermoelastic signal as follows:

$$\Delta\varepsilon_L + \Delta\varepsilon_T = B^* S_c \quad (16)$$

If the material is thermoelastically orthotropic for lay-ups where the principal material axes and the surface ply axes correspond it is possible the following equation can be used as a basis for calibration:

$$\frac{\Delta\varepsilon_L((\alpha_1 Q_{11} + \alpha_2 Q_{12}) - \nu_{LT}(\alpha_1 Q_{12} + \alpha_2 Q_{22}))}{S} = A^* \quad (17)$$

Clearly it is not possible to manipulate Eq. (17) to give a simple expression that relates the strain to the thermoelastic signal. In cases when  $\nu_{LT} \rightarrow 0$ , e.g. cross ply laminates it would be possible to neglect the second bracketed term in the numerator of Eq. (17) as in these cases the transverse strain is small. In other cases it is necessary to measure both the longitudinal strain and the transverse strain and know the material properties given in Eq. (17), so the calibration would determine  $A^*$  only.

## 6. Conclusions

The motivation for the work presented here was the development of a calibration routine so that quantitative stress or strain values can be obtained from a general composite structure. It has been shown that a traditional stress based calibration routine is dependent on knowledge of the stresses in the surface lamina, which for a general composite laminate must be calculated using CLT that necessitates an accurate knowledge of the material properties. The paper has shown that obtaining the relevant material properties requires a large experimental coverage so a revised calibration routine based on the measurement of the laminate strains was devised. The revised calibration routine has been presented and validated by investigating the thermoelastic response from test specimens with a variety of stacking sequences. This revealed that the thermoelastic response was from the isotropic resin-rich layer, which was only 25  $\mu\text{m}$  thick. Therefore a new calibration constant  $B^*$  has been proposed for test specimens with resin-rich layer based on an isotropic thermoelastic response from specimens that are mechanically orthotropic and a further calibration constant for specimens without a resin-rich surface layer that are mechanically and thermoelastically orthotropic. In the procedure the calibration constants are obtained by measuring the laminate strain, from a tensile calibration coupon, using a surface mounted extensometer and combining this with the measured thermoelastic response.

## Acknowledgements

The thermoelastic data collected in this work was obtained using a Deltatherm 1000 system borrowed from the UK Engineering and Physical Sciences Research Council (EPSRC) loan pool.

## References

- [1] Dulieu-Barton JM, and Stanley P. Development and applications of thermoelastic stress analysis. *J Strain Anal Eng.* 1998; **33**(2): 93-104.
- [2] Quinn S, Dulieu-Barton JM, and Langlands JM. Progress in thermoelastic residual stress measurement. *Strain.* 2004; **40** (3): 127- 133.
- [3] Diaz FA, Patterson EA, Tomlinson RA, Yates JR. Measuring stress intensity factors during fatigue crack growth using thermoelasticity. *Fatigue Fract Eng M.* 2004; **27**(7): 571-584.
- [4] Lin ST, Miles JP, Rowlands RE. Image enhancement and stress separation of thermoelastically measured data under random loading. *Exp Mech* 1997; **37**(3).
- [5] Pitarresi G, Patterson EA. A review of the general theory of thermoelastic stress analysis. *J Strain Anal Eng.* 2003; **38**(5): 405-417.
- [6] Stanley P, Chan WK. Quantitative stress analysis by means of the thermoelastic effect. *J Strain Anal Eng* 1984; **20** (3):129-137
- [7] Dulieu-Smith JM. Alternative calibration techniques for quantitative thermoelastic stress analysis. *Strain* 1995; **31**(1): 9-16.
- [8] Whelan M, Hack E, Siebert T, Burguete R, Patterson E, Salem Q. On the calibration of optical full-field strain measurement systems. *Applied Mechanics and Materials* 2005; **3-4**: 397-402.
- [9] Stanley P, Chan WK. The application of thermoelastic stress analysis to composite materials. *J Strain Anal Eng* 1988; **23**(3): 137-142.
- [10] Potter RT. Stress analysis in laminated fibre composites by thermoelastic emission. In: Proceedings of the 2<sup>nd</sup> international conference on stress analysis by thermoelastic techniques, SPIE vol. 731, London, 1987
- [11] Bakis CE, Reifsnider KL. The adiabatic thermoelastic effect in laminated fiber composites. *J Compos Mater* 1991; **25**: 809-830.

- [12] Wong AK, A non-adiabatic thermoelastic theory for composite laminates. *J Phys Chem Solid* 1991; **52**(3): 483-494.
- [13] Cunningham PR, Dulieu-Barton JM, Dutton AG, Shenoi RA. The effect of ply lay-up on the thermoelastic response of laminated composites. *Key Eng Mat* 2002; **221-222**: 325-336.
- [14] El-Hajjar R, Haj-Ali R. A quantitative thermoelastic stress analysis method for pultruded composites. *Comp Sci Tech* 2003; **63**(7): 967-978.
- [15] Pitarresi G, Found MS, Patterson EA. An investigation of the influence of macroscopic heterogeneity on the thermoelastic response of fibre reinforced plastics. *Comp Sci Tech* 2005; **65**(2): 269-280.
- [16] Dulieu-Smith JM, Quinn S, Shenoi RA, Read PJCL, Moy SSJ. Thermoelastic stress analysis of a GRP tee joint. *App Compos Mater* 1997; **4**(5): 283-303.
- [17] Dulieu-Barton JM, Earl JS, Shenoi RA. Determination of the stress distribution in foam-cored sandwich construction composite tee joints. *J Strain Anal Eng* 2001; **36**(6): 545-560.
- [18] Boyd SW, Dulieu-Barton JM, Rumsey L. Stress analysis of finger joints in pultruded GRP material. *Int J Adhes Adhes* 2006; **26**(7): 498-510.
- [19] Daniel IM. Failure of composite materials. *Strain* 2007; **43**(1): 4-12.
- [20] Daniel IM, Ishai O. *Engineering Mechanics of Composite Materials*. Oxford: Oxford University Press; 1994.
- [21] Rogers GFC, Mayhew Y R. *Engineering Thermodynamics: Work and Heat Transfer*. Fourth ed. Longman; 1992.
- [22] Dulieu-Barton JM, Emery TR, Quinn S, Cunningham PR. A temperature correction methodology for quantitative thermoelastic stress analysis and damage assessment. *Meas Sci Technol* 2006; **17**(6): 1627-1637.
- [23] Standard Test Method for Tensile Properties of Fiber-Resin Composites. American Society for Testing and Materials (ASTM) D3039-76. 1989.
- [24] Dato M. *Mechanics of Fibrous Composites*, Elsevier Applied Science. 1991
- [25] Harwood N, Cummings WM. *Thermoelastic Stress Analysis*. Adam Hilger. 1991
- [26] Technical Data 135 Resin/229 Hardener. Pro-Set Inc. 2007
- [27] Dulieu-Smith JM, Stanley P. On the interpretation and significance of the Grüneisen parameter in

thermoelastic stress analysis. *J Mater Process Tech* 1998; **78**(1): 75-83.

[28] Personal communication with Gurit. Newport, Isle of Wight, U.K.

[29] Lesniak JR, Boyce BR, Sandor BI. Thermographic stress analysis / NDE via focal-plane array detectors. NASA Contract Report CR-NASA-19262. 1991

[30] Kalogiannakis G, Hemelrijck DV, Assche, GV. Measurements of Thermal Properties of Carbon/Epoxy and Glass/Epoxy using Modulated Temperature Differential Scanning Calorimetry. *J Compos Mater* 2004; **38**(2): 163-175.

[31] Lubin G. Handbook of fibreglass and advanced plastic composites. New York: Van Nostrand Reinhold Co. Ltd.; 1969.

### Figure Captions

Fig. 1. Laminate schematic (all measurements in millimetres)

Fig. 2. Micrograph of UD laminate

**Table 1 Laminate notation, geometry, stacking sequence and thermoelastic calibration**

Notation	Thickness (mm)	Length (mm)	Stacking sequence	Calibration constant
UD	3.5	181	[0] <sub>13</sub>	$A^* = \{[(\alpha_1 Q_{11} + \alpha_2 Q_{12}) - \nu_{LT}(\alpha_1 Q_{12} + \alpha_2 Q_{22})] \Delta \epsilon_L\} / S$
Mixed	3.56	183	[(0 <sub>6</sub> , 90, 0, 90, 0 <sub>6</sub> )]	$A^* = \{[(\alpha_1 Q_{11} + \alpha_2 Q_{12}) - \nu_{LT}(\alpha_1 Q_{12} + \alpha_2 Q_{22})] \Delta \epsilon_L\} / S$
0/90	3.55	182.5	[(0/90) <sub>3,0</sub> , (90/0) <sub>3</sub> ]	$A^* = \{[(\alpha_1 Q_{11} + \alpha_2 Q_{12}) - \nu_{LT}(\alpha_1 Q_{12} + \alpha_2 Q_{22})] \Delta \epsilon_L\} / S$
90/0	3.561	179.5	[(90/0) <sub>3,0</sub> , (0/90) <sub>3</sub> ]	$A^* = \{[(\alpha_1 Q_{12} + \alpha_2 Q_{22}) - \nu_{LT}(\alpha_1 Q_{11} + \alpha_2 Q_{12})] \Delta \epsilon_L\} / S$
± 45	3.587	182	[(+45/-45) <sub>3,45</sub> , (+45/-45) <sub>3</sub> ]	$A^* = \{((\alpha_1 Q_{11} + \alpha_2 Q_{12}) + (\alpha_1 Q_{12} + \alpha_2 Q_{22}))(\Delta \epsilon_L + \Delta \epsilon_T) + (((\alpha_1 Q_{11} + \alpha_2 Q_{12}) - (\alpha_1 Q_{12} + \alpha_2 Q_{22})) \gamma_{LT})\} / 2S$
Resin-rich layer	As specimens above	As specimens above	As specimens above	$A^* = \left[ \left( \frac{\alpha_R E_R}{1 - \nu_R} (1 - \nu_{LT}) \right) \Delta \epsilon_L \right] / S$

where  $\alpha_R$  is the coefficient of thermal expansion of the resin-rich layer,  $E_R$  is the Young's modulus and  $\nu_R$  the Poisson's ratio of the resin-rich layer

**Table 2 Loading regimes**

Laminate index	Constant load (8 kN)	Constant displacement (0.44 mm)
	Displacement applied (mm)	Load range (kN)
UD	0.32	10.99
Mixed	0.34	10.40
0/90	0.44	8.00
90/0	0.48	7.48
± 45	1.2	3.28

**Table 3 Unidirectional E-Glass/epoxy material properties**

Longitudinal Young's modulus, $E_1$ (GPa)	36.8
Transverse Young's modulus, $E_2$ (GPa)	8.4
Shear modulus, $G_{12}$ (GPa)	3 [25]
Major Poisson's ratio, $\nu_{12}$	0.25
Minor Poisson's ratio, $\nu_{21}$	0.05
Coefficient of thermal expansion, $\alpha_1$ ( $^{\circ}\text{C}$ )	$6 \times 10^{-6}$ [25]
Coefficient of thermal expansion, $\alpha_2$ ( $^{\circ}\text{C}$ )	$35 \times 10^{-6}$ [25]
Specific heat, $C_p$ (J/kg K)	882 [30]
Density, $\rho$ ( $\text{kg/m}^3$ )	1846 [13]

**Table 4 Epoxy material properties**

Young's modulus, $E_R$ (GPa)	3.7 GPa [26]
Poisson's ratio, $\nu_R$	0.40 [27]
Coefficient of thermal expansion, $\alpha$ ( $^{\circ}\text{C}$ )	$65 \times 10^{-6}$ [28]
Specific heat, $C_p$ (J/kg K)	1040 [30]
Density, $\rho$ ( $\text{kg/m}^3$ )	1170 [27]
Emissivity	0.79 [31]

**Table 5 Laminate properties**

Specimen	CLT		Experimental	
	Young's modulus, $E_L$ (MPa)	Poisson's ratio, $\nu_{LT}$	Young's modulus, $E_L$ (MPa)	Poisson's ratio, $\nu_{LT}$
UD	36.8	0.25	36.8	0.25
90	8.4	0.05	8.4	0.05
Mixed	33.6	0.16	31.9	0.14
0/90	24.5	0.096	23.5	0.099
90/0	22.2	0.087	20.9	0.083
$\pm 45$	9.2	0.60	9.0	0.49

**Table 6 Applied stress and strain values for the load control tests**

Laminate	Method	UD	Mixed	0/90	90/0	$\pm 45$
<i>Orthotropic surface layer</i>						
$\Delta\sigma_1$ (MPa)	CLT	57.3	64.9	88.9	-3.3	41.8
$\Delta\sigma_2$ (MPa)	CLT	0	1.2	3.1	22.0	13.8
<i>Resin-rich layer</i>						
$\Delta\sigma_x$ (MPa)	CLT	6.2	7.7	10.1	11.3	20.0
$\Delta\sigma_y$ (MPa)	CLT	1.0	1.8	3.2	3.6	-4.9
<i>Laminate</i>						
$\Delta\varepsilon_L$	CLT	0.00156	0.00176	0.00240	0.00265	0.00577
$\Delta\varepsilon_T$	CLT	-0.000393	-0.000297	-0.000239	-0.000239	-0.00348
$\Delta\varepsilon_L$	Measured	0.00155	0.00179	0.00231	0.00252	0.00530
$\Delta\varepsilon_T$	Measured	-0.000373	-0.000251	-0.000228	-0.000209	-0.00352

**Table 7 Applied stress and strain values for the displacement control tests**

Laminate	Method	UD	Mixed	0/90	90/0	±45
<i>Orthotropic surface layer</i>						
$\Delta\sigma_1$ (MPa)	CLT	78.7	84.4	88.9	-3.0	15.6
$\Delta\sigma_2$ (MPa)	CLT	0	1.6	3.1	20.6	5.5
<i>Resin-rich layer</i>						
$\Delta\sigma_x$ (MPa)	CLT	8.5	9.4	10.1	10.5	8.0
$\Delta\sigma_y$ (MPa)	CLT	1.4	2.3	3.2	3.4	-2.25
<i>Laminate</i>						
$\Delta\epsilon_L$	CLT	0.00214	0.00229	0.00240	0.00248	0.00237
$\Delta\epsilon_T$	CLT	-0.00054	-0.000386	-0.000239	-0.000223	-0.00144
$\Delta\epsilon_L$	Measured	0.00219	0.00222	0.00235	0.00241	0.00215
$\Delta\epsilon_T$	Measured	-0.000527	-0.000311	-0.000232	-0.000200	-0.00105

**Table 8 Thermoelastic signal, S**

Laminate	UD	Mixed	0/90	90/0	±45
<i>S (load)</i>	585 ± 7.3 %	765 ± 4.7 %	1136 ± 4.5 %	1189 ± 5.8 %	1105 ± 5.8 %
<i>S (displacement)</i>	845 ± 7.4 %	999 ± 4.9 %	1136 ± 4.9 %	1169 ± 5.7 %	460 ± 7.9 %

**Table 9 A\* derived for orthotropic surface ply properties (Constant load)**

	UD	Mixed	0/90	90/0	±45
i) (MPa/°C)	0.589	0.565	0.564	0.630	0.613
ii) (MPa/°C)	0.589	0.574	0.564	0.620	0.621
iii) (MPa/°C)	0.595	0.599	0.543	0.595	0.614

**Table 10 A\* derived for orthotropic surface ply properties (Constant displacement)**

	UD	Mixed	0/90	90/0	±45
i) (MPa/°C)	0.559	0.563	0.564	0.601	0.601
ii) (MPa/°C)	0.560	0.560	0.564	0.598	0.616
iii) (MPa/°C)	0.568	0.585	0.566	0.579	0.610

**Table 11 A\* derived for isotropic resin-rich layer properties (Constant load)**

	UD	Mixed	0/90	90/0	±45
i) (MPa/°C)	0.799	0.808	0.759	0.816	0.888
ii) (MPa/°C)	0.807	0.781	0.772	0.813	0.835
iii) (MPa/°C)	0.814	0.814	0.737	0.784	0.884

**Table 12 A\* derived for isotropic resin-rich layer properties (Constant displacement)**

	UD	Mixed	0/90	90/0	±45
i) (MPa/°C)	0.761	0.757	0.759	0.772	0.814
ii) (MPa/°C)	0.766	0.778	0.772	0.778	0.797
iii) (MPa/°C)	0.780	0.763	0.768	0.763	0.826

**Table 13 Thermoelastic temperature change obtained for resin-rich layer**

Test method		$\Delta T$ (°C)				
		UD	Mixed	0/90	90/0	$\pm 45$
Load	Calculated	0.112	0.148	0.206	0.232	0.240
	Measured	0.10	0.13	0.18	0.21	0.25
Displacement	Calculated	0.154	0.182	0.206	0.216	0.09
	Measured	0.14	0.17	0.19	0.19	0.09

**Table 14 Thermoelastic temperature change obtained for orthotropic surface ply**

Test method		$\Delta T$ (°C)				
		UD	Mixed	0/90	90/0	$\pm 45$
Load	Calculated	0.061	0.077	0.115	0.134	0.131
	Measured	0.10	0.13	0.18	0.21	0.25
Displacement	Calculated	0.084	0.10	0.115	0.126	0.051
	Measured	0.14	0.17	0.19	0.19	0.09

**Table 15  $B^*$  values for each test specimen**

		UD	Mixed	0/90	90/0	$\pm 45$
$B^*$	Constant load	0.199	0.190	0.190	0.200	0.204
$B^*$	Constant displacement	0.190	0.189	0.190	0.192	0.198

Fig.1

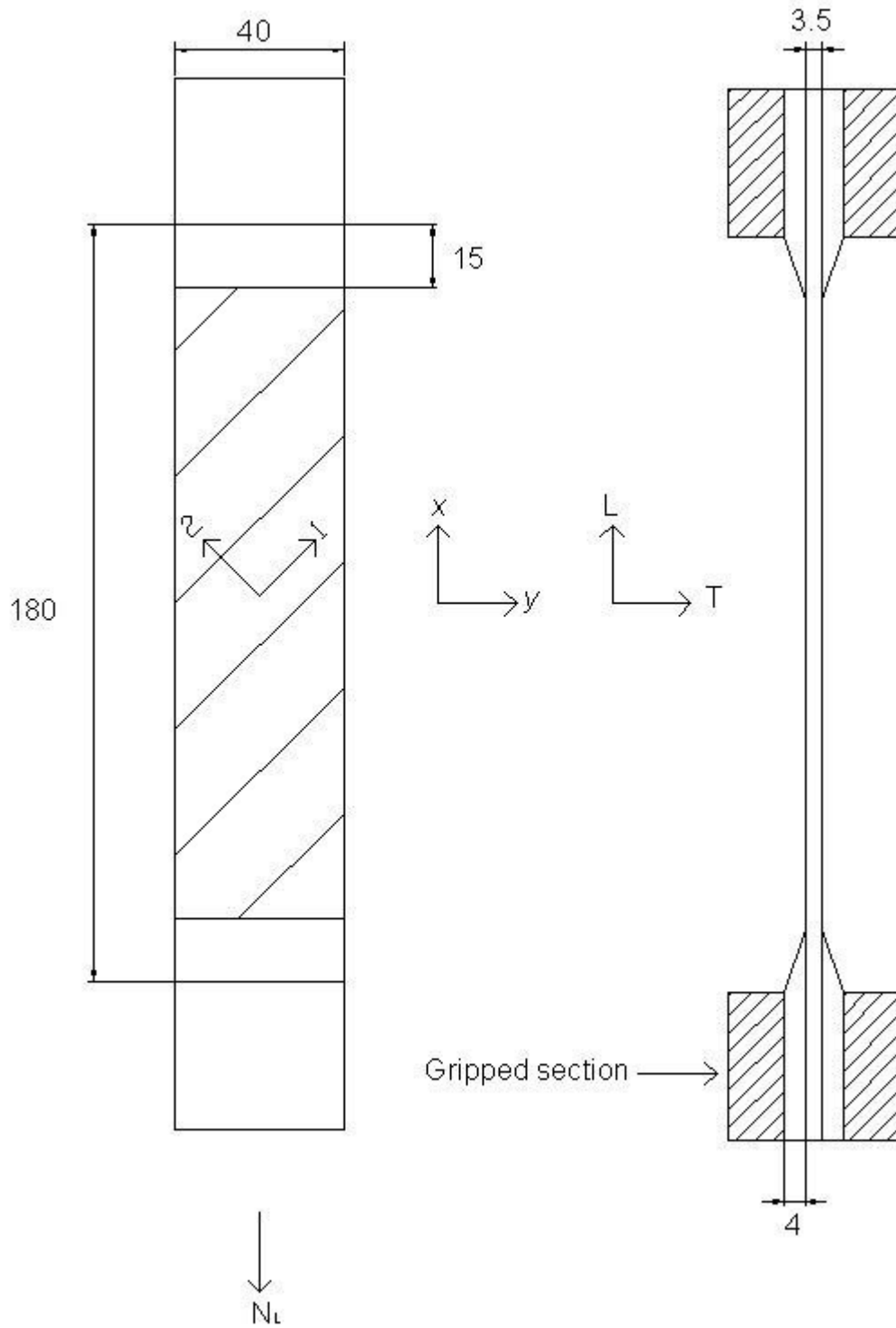
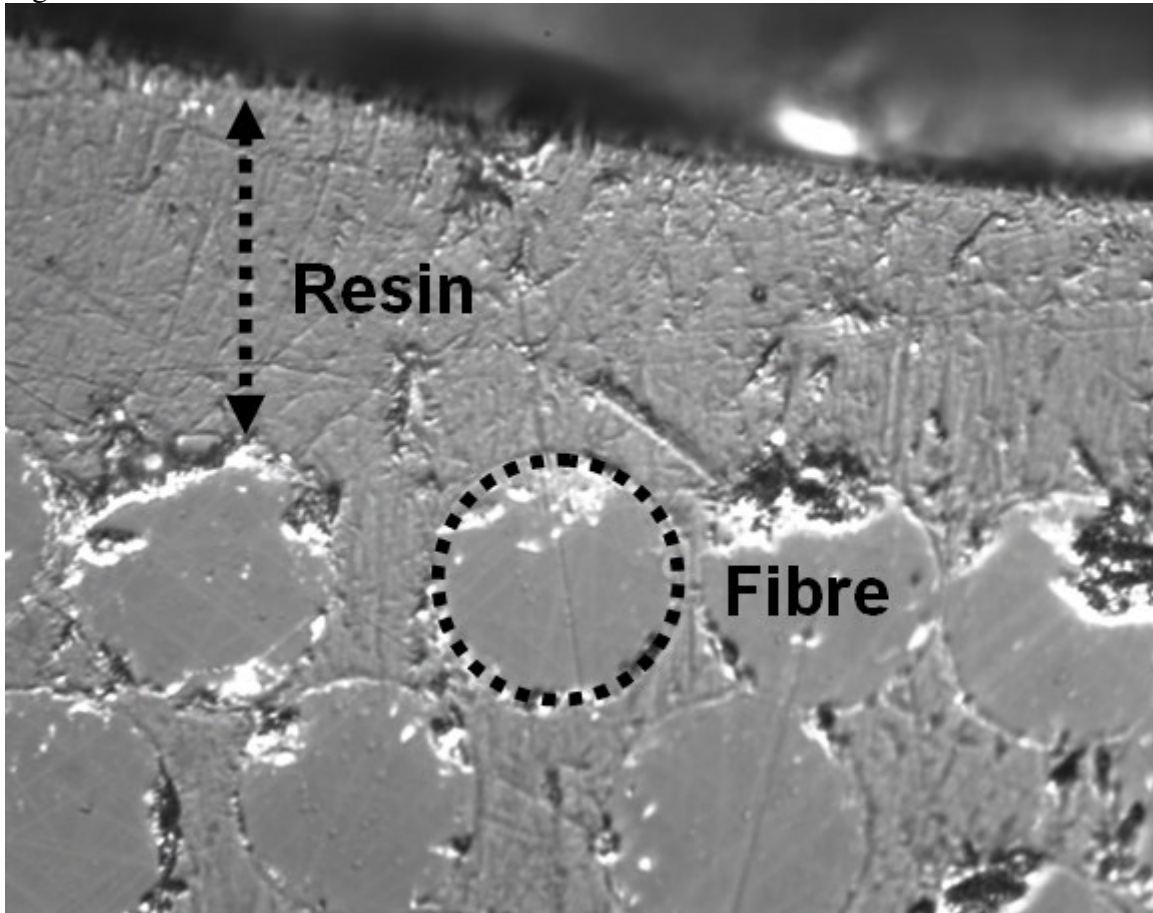


Fig.2



ACCEPTED